

Incarceration of (PdO)_n and Pd_n Clusters by Cage-Templated Synthesis of Hollow Silica Nanoparticles**

Kiyotaka Takao, Kosuke Suzuki, Tatsuya Ichijo, Sota Sato, Hiroyuki Asakura, Kentaro Teramura, Kazuo Kato, Tomonori Ohba, Takeshi Morita, and Makoto Fujita*

Metal nanoclusters have recently attracted considerable interest because of their distinct chemical and physical properties, such as catalytic activities,^[1] optical properties,^[2] and magnetic behavior,^[3] which are different from those of both bulk materials and mononuclear metal species. When the number of metal centers (*n*) is small, the properties of the metal clusters (M_n) change dramatically with increasing *n* value. Therefore, intense efforts have been made to synthesize small-numbered, well-defined clusters with non-distributed *n* values. Gas-phase preparation by metal vaporization is a promising physical method to prepare small-numbered M_n clusters (typically in the range of *n* = 10–10000).^[4] Solution synthesis through the reduction of metal ion precursors within templates is also an efficient method to give M_n clusters of similar size.^[5] With all of these methods it is still difficult to strictly control the number of metal centers particularly when *n* is around 10 or less. Furthermore, the resulting synthesized clusters are often chemically and physically labile and are quite prone to oxidation or fusing into larger clusters. The most controllable methods to synthesize metal clusters with small *n* values (*n* = 4–60) have been reported utilizing the voids of dendrimers,^[1a,c,6] but this method is hampered by the tedious dendrimer synthesis. Herein, we report a unique approach to incarcerated metal clusters with strictly controlled *n* values (ca. 12) within hollow

silica nanoparticles. Our method utilizes a Pd₁₂L₂₄ spherical complex^[7] as a template for the hollow silica synthesis. After sol-gel condensation around the sphere, the incarcerated Pd₁₂L₂₄ core is calcinated to give (PdO)_n oxide clusters and subsequently reduced to Pd_n metal clusters (Figure 1). X-ray absorption fine structure (XAFS) analysis indicated that the

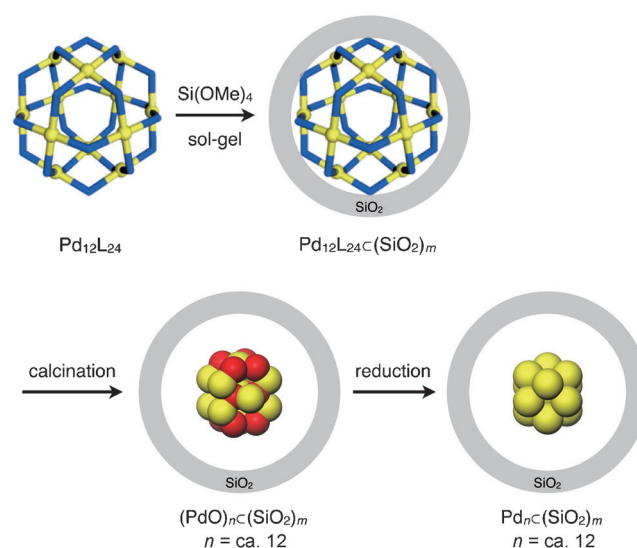


Figure 1. Preparation of (PdO)_n and Pd_n cluster-incarcerated silica nanoparticles (*n* = ca. 12).

(PdO)_n and Pd_n clusters prepared in situ are strictly controlled with *n* = ca. 12, because the Pd₁₂L₂₄ precursors are completely isolated from each other by the hollow silica and have no opportunity to fuse into larger clusters during calcination and reduction. All of the metal-incarcerated hollow silica nanoparticles have been well characterized by transmission electron microscopy (TEM), X-ray photoelectron spectroscopy (XPS), and/or XAFS to demonstrate that our strategy provides a unique and highly effective method for cluster synthesis with a limited number of metal atoms.

For the spherical Pd₁₂L₂₄ precursor **2**, we designed bent ligand **1** with a triethoxysilyl group at the convex (Figure 2 a). The alkoxysilyl group is essential in initiating the sol-gel condensation of the Si(OMe)₄ monomer at the periphery of the sphere. Ligand **1** was synthesized in high yield in three steps from 3,5-dibromophenol: 1) Williamson reaction with 4-bromo-1-butene, 2) Suzuki–Miyaura cross coupling with 4-pyridylboronic acid pinacol ester, and 3) hydrosilylation with HSi(OEt)₃. When ligand **1** (5.0 μmol) was treated with

[*] K. Takao, Dr. K. Suzuki, T. Ichijo, Dr. S. Sato, Prof. Dr. M. Fujita
Department of Applied Chemistry, School of Engineering
The University of Tokyo
7-3-1 Hongo, Bunkyo-ku, Tokyo 113-8656 (Japan)
E-mail: mfujita@appchem.t.u-tokyo.ac.jp

H. Asakura, Dr. K. Teramura
Department of Molecular Engineering, Graduate School of
Engineering, Kyoto University
Kyotodaigaku Katsura, Nishikyo-ku, Kyoto 615-8510 (Japan)

Dr. K. Kato
Japan Synchrotron Radiation Research Institute
1-1 Kouto, Sayo-cyo, Sayo-gun, Hyogo 679-5198 (Japan)

Dr. T. Ohba
Graduate School of Science, Chiba University
1-33 Yayoi-cho, Inage-ku, Chiba 263-8522 (Japan)

Dr. T. Morita
Graduate School of Advanced Integration Science, Chiba University
1-33 Yayoi-cho, Inage-ku, Chiba 263-8522 (Japan)

[**] This research was supported by the JST-CREST project, for which M.F. is the principal investigator, and also in part by KAKENHI and MEXT. Synchrotron XAFS studies were performed at SPring-8, and TEM studies were performed at Chiba University and at the University of Tokyo.

Supporting information for this article is available on the WWW under <http://dx.doi.org/10.1002/anie.201201288>.

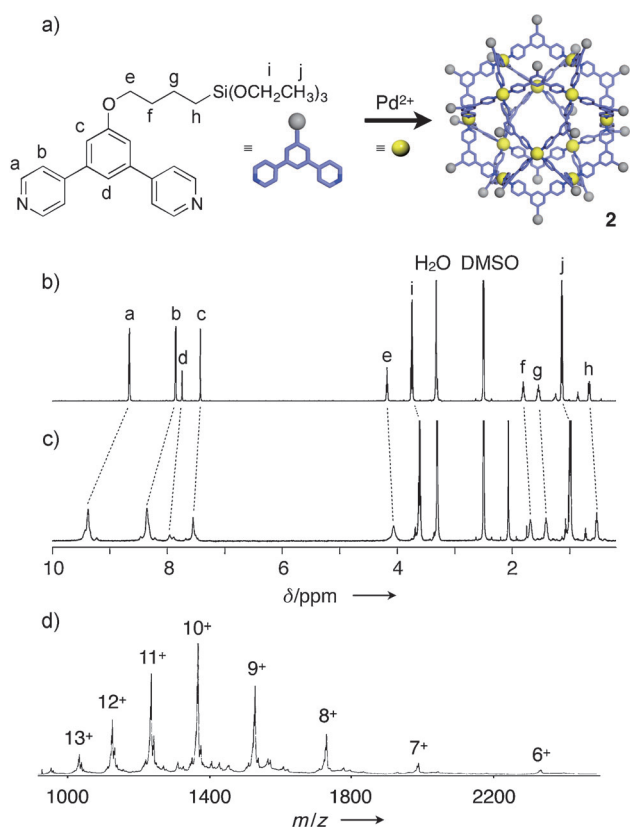


Figure 2. Preparation of $\text{Pd}_{12}\text{L}_{24}$ precursor **2**. a) Synthesis of **2** from ligand **1** and Pd^{II} ions. b, c) ^1H NMR spectra (500 MHz, 27°C , $[\text{D}_6]\text{DMSO}$) of b) ligand **1** and c) complex **2**. d) CSI mass spectrum of **2** ($\text{DMSO}/\text{CH}_3\text{CN} = 1:24$).

$\text{Pd}(\text{BF}_4)_2$ (2.6 μmol) in DMSO (0.52 mL) at 50°C for 1 h, a $\text{Pd}_{12}\text{L}_{24}$ sphere with 24 alkoxysilyl groups at the periphery of the sphere was quantitatively formed. In the ^1H NMR spectrum, the α and β protons on the pyridyl groups (PyH_α and PyH_β) are shifted downfield owing to coordination to Pd ions ($\Delta\delta = 0.72$ and 0.51 ppm for PyH_α and PyH_β , respectively, Figure 2b,c). Diffusion-ordered NMR spectroscopy (DOSY) showed a diffusion coefficient of $D = 4.0 \times 10^{-11} \text{ m}^2 \text{ s}^{-1}$ in $[\text{D}_6]\text{DMSO}$, which indicates the formation of a huge molecule. This result is comparable to those of related $\text{Pd}_{12}\text{L}_{24}$ spheres, but considerably smaller than that of the component ligand ($D = 1.8 \times 10^{-10} \text{ m}^2 \text{ s}^{-1}$ in $[\text{D}_6]\text{DMSO}$). The visible signal broadening is also indicative of the formation of a huge molecule (Figure 2b,c). The $\text{Pd}_{12}\text{L}_{24}$ composition was determined by cold-spray ionization (CSI) mass spectrometry with prominent peaks for $[\mathbf{2}-(\text{BF}_4^-)_a]^{a+}$ ($a = 13\text{--}6$; Figure 2d).

To incarcerate sphere **2** within a hollow silica nanoparticle, the sol-gel condensation of tetramethoxysilane (TMOS) at the periphery of **2** was carried out (Figure 3a). A DMSO solution of sphere **2** (0.30 mM, 80 μL) was diluted with methanol (0.72 mL) and then TMOS (2000 equiv), water (50000 equiv), and nitric acid (4.2 equiv) were added. The reaction was monitored by NMR spectroscopy (Figure 3b). The signals derived from the core of **2** gradually broadened, indicating the formation of a silica layer around the periphery of **2**. Despite the use of a large excess of TMOS (2000 equiv),

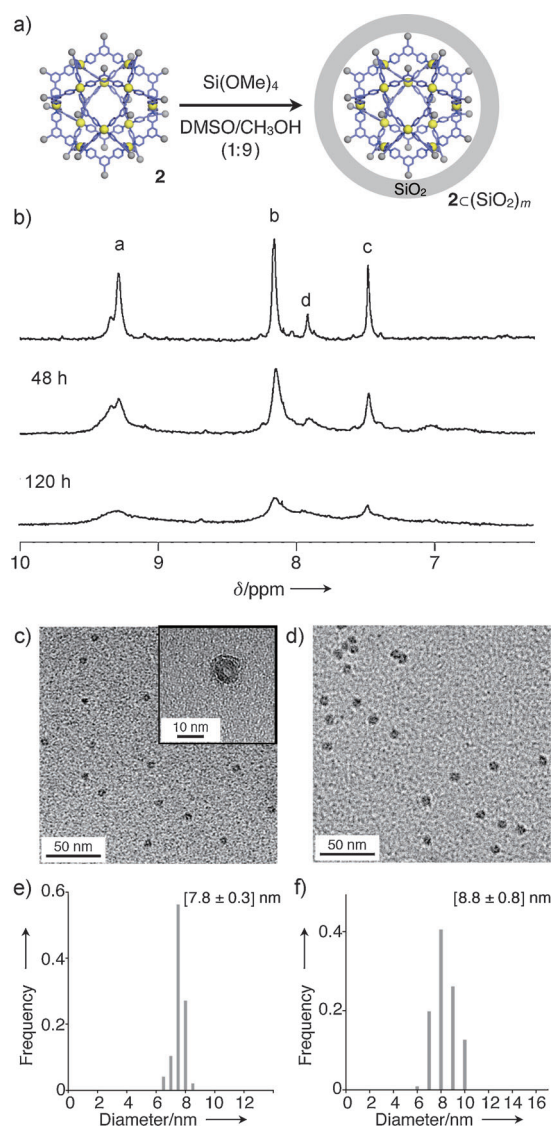


Figure 3. Template synthesis of a $\text{Pd}_{12}\text{L}_{24}$ complex incarcerated in a hollow silica nanoparticle **2**. a) Synthesis of $2\text{C}(\text{SiO}_2)_m$ by the sol-gel condensation of $\text{Si}(\text{OMe})_4$ around the template **2**. b) ^1H NMR (500 MHz, 27°C , $[\text{D}_6]\text{DMSO}/\text{CD}_3\text{OD}/\text{D}_2\text{O} = 4:36:1$) observation of the conversion of **2** into $2\text{C}(\text{SiO}_2)_m$; the spectrum at the top is before addition of $\text{Si}(\text{OMe})_4$; the middle and bottom spectra are 48 h and 120 h after addition of $\text{Si}(\text{OMe})_4$ (2000 equiv), respectively. c, d) TEM images of hollow silica nanoparticles c) $2\text{C}(\text{SiO}_2)_{2000}$ and d) $2\text{C}(\text{SiO}_2)_{7200}$. The inset in (c) is the magnified image of a hollow silica nanoparticle. e, f) Size distribution determined from the TEM images of e) $2\text{C}(\text{SiO}_2)_{2000}$ and f) $2\text{C}(\text{SiO}_2)_{7200}$.

bulk silica gels did not precipitate and the solution remained clear even after 5 days. Thus, the sol-gel condensation seems to proceed only around sphere **2**. The formation of the silica nanoparticle incarcerating **2** (which is hereafter presented as $2\text{C}(\text{SiO}_2)_{2000}$) is strongly indicated by DOSY, which shows a single product with a diffusion coefficient of $D = 5.6 \times 10^{-11} \text{ m}^2 \text{ s}^{-1}$ in the mixed solvent, a value which is considerably smaller than that of sphere **2** ($D = 1.3 \times 10^{-10} \text{ m}^2 \text{ s}^{-1}$) in the same solvent mixture and consistent with the increased molecular size caused by the silica coating. Even when the amount of TMOS was increased (7200 equiv), the condensa-

tion proceeded without silica-gel precipitation to form a much larger silica-coated sphere ($2\text{C}(\text{SiO}_2)_{7200}$). As the ^1H NMR signals were heavily broadened, clear signals were not observed in DOSY and the diffusion coefficient was no longer measurable. The presence of the $\text{Si}(\text{OEt})_3$ group on the ligand is essential to the initiation of the sol-gel condensation at the periphery of the sphere: when the $\text{Si}(\text{OEt})_3$ groups were absent, the condensation occurred in bulk solution and silica gel precipitated while the spherical complex remained intact.

TEM observation showed highly dispersed nanoparticles with a very narrow size distribution: the diameters of $2\text{C}(\text{SiO}_2)_{2000}$ and $2\text{C}(\text{SiO}_2)_{7200}$ were estimated to be $[7.8 \pm 0.3]$ and $[8.8 \pm 0.8]$ nm, respectively (Figure 3 c,d). More importantly, the TEM showed a clear contrast in the hollows at the center of the silica nanoparticles (inset in Figure 3 c). From the TEM image, the diameter of the hollows is ca. 3 nm, a value consistent with the diameter of the $\text{Pd}_{12}\text{L}_{24}$ spherical shell (3.5 nm). Presumably, the highly accumulated $\text{Si}(\text{OEt})_3$ groups at the periphery of the sphere initiated the condensation predominantly at the surface of the sphere, forming a thin layer of silica on the surface. Once the layer was formed, the TMOS monomers could no longer enter the spherical shell and further condensation occurred only on the surface, giving the hollow structure.

It is noteworthy that the hollow silica incarcerates a single 3.5 nm-sized $\text{Pd}_{12}\text{L}_{24}$ spherical complex. Because of this fact, we expected that a Pd_{12} cluster could be formed by removal of the ligands without breaking the hollow structure of the silica. Thus, the silica nanoparticle $2\text{C}(\text{SiO}_2)_{7200}$ was precipitated by removing the MeOH solvent and adding poor solvents (ethyl acetate and ether). The precipitated $2\text{C}(\text{SiO}_2)_{7200}$ powder was calcinated at 400°C for 2 h in air.

For the calcinated powder, XPS analyses were performed to determine the valence state of the Pd atoms. The core-level $\text{Pd } 3d_{3/2}$ and $3d_{5/2}$ peaks of $(\text{PdO})_n\text{C}(\text{SiO}_2)_{7200}$ were observed at 341.3 and 336.2 eV, respectively. The comparison of the values to those of Pd foil and PdO as reference samples showed the oxidized state of the Pd atoms, a result consistent with the formation of $(\text{PdO})_n\text{C}(\text{SiO}_2)_{7200}$ (Figure 4a). To determine if $(\text{PdO})_n$ clusters were incarcerated in the silica capsule, the surface of $(\text{PdO})_n\text{C}(\text{SiO}_2)_{7200}$ was sputtered

with a Xe beam at 3 kV followed by XPS experiments at every 0.1 min. The peak intensities of the Pd 3d XPS increased as Xe sputtering proceeded, and the binding energy shifted to lower energy as the duration of X-ray irradiation increased, which indicates that some of the $(\text{PdO})_n$ clusters were reduced by X-ray irradiation. As shown in Figure 4b, the Pd/Si molar ratio, as evaluated by comparison of Pd 3d and Si 2p peaks, increased with increasing sputtering duration and reached a maximum of 0.35 % after 0.4 min. Further sputtering had no effect on the Pd/Si ratio. This behavior indicates that the silica shell was destroyed by the heavy Xe ion for the first 0.4 min of the sputtering and that the Pd species was then exposed on the surface, at which time the Pd/Si ratio on the surface became constant. This observation supports the existence of $(\text{PdO})_n$ clusters inside the silica capsule.

Structural details of the $(\text{PdO})_n\text{C}(\text{SiO}_2)_{7200}$ were elucidated by XAFS at the K-edge of Pd. The X-ray absorption near edge structure (XANES) spectra of the $(\text{PdO})_n$ cluster and those of Pd foil and PdO as reference samples showed

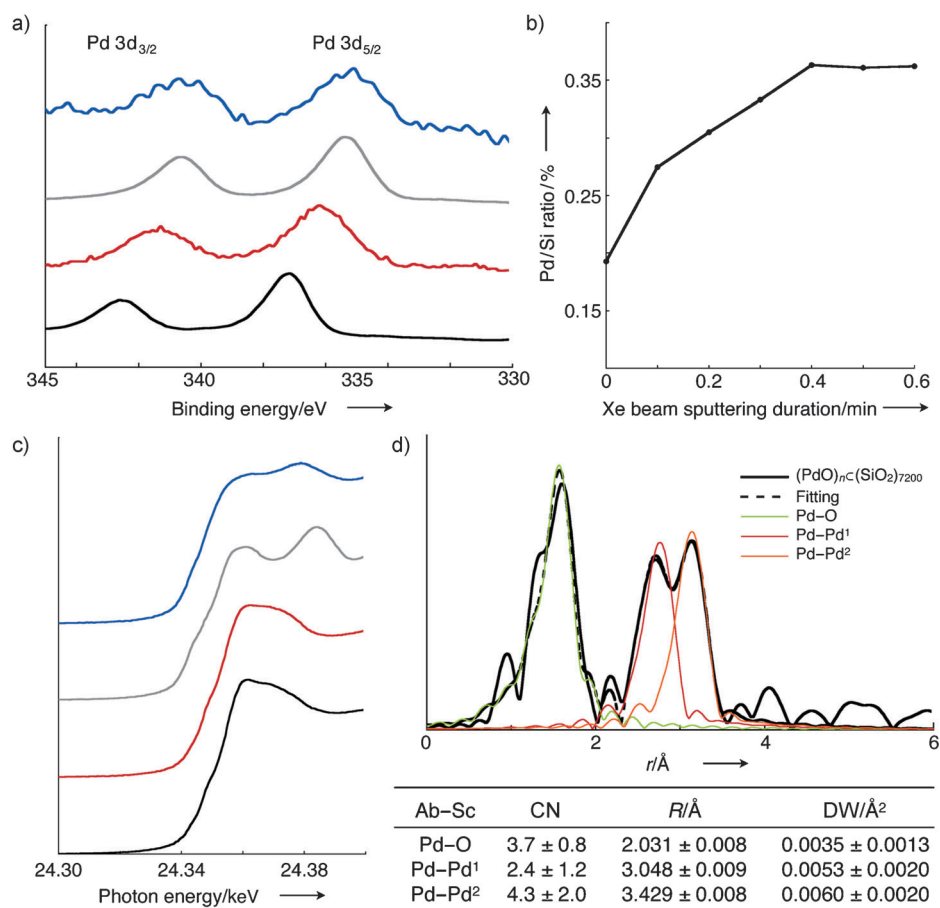


Figure 4. XPS analyses of $(\text{PdO})_n\text{C}(\text{SiO}_2)_{7200}$ and $\text{Pd}_n\text{C}(\text{SiO}_2)_{7200}$. a) Pd 3d XPS spectra of PdO (—), $(\text{PdO})_n\text{C}(\text{SiO}_2)_{7200}$ (—), Pd foil (—), and $\text{Pd}_n\text{C}(\text{SiO}_2)_{7200}$ (—). b) Time course of the Pd/Si ratio of $(\text{PdO})_n\text{C}(\text{SiO}_2)_{7200}$ during surface sputtering by a Xe beam for a duration of 0.6 min. c) Pd K-edge XANES spectra of PdO (—), $(\text{PdO})_n\text{C}(\text{SiO}_2)_{7200}$ (—), Pd foil (—), and $\text{Pd}_n\text{C}(\text{SiO}_2)_{7200}$ (—). d) Curve fitting result of the Fourier transformation of the EXAFS of $(\text{PdO})_n\text{C}(\text{SiO}_2)_{7200}$; $\Delta k = 2\text{--}15 \text{ \AA}^{-1}$, $\Delta R = 1.4\text{--}3.4 \text{ \AA}$. Curve fitting was performed by Artemis with back scattering and phase shift parameters calculated by FEFF ver. 8.40, and fell within the Nyquist criteria. Curve fitting was done in *R* space (*R*-factor=0.01078). CN = coordination number, DW = Debye-Waller factor.

that the valence state of the Pd atoms in $(\text{PdO})_n$ is divalent, a result which is consistent with the XPS experiments (Figure 4c). Extended X-ray absorption fine structure (EXAFS) experiments were performed to estimate the value of n for $(\text{PdO})_n$. The coordination number (CN) and the atomic distance (d) were determined by curve fitting analyses for adjacent X-ray absorbing and scattering atom pairs (Ab–Sc) of Pd–O and Pd–Pd (Figure 4d). The experimental CN and d values were reasonable for the structure of a $(\text{PdO})_n$ cluster where n is ca. 12. The $(\text{PdO})_n$ clusters derived from $\text{Pd}_{12}\text{L}_{24}$ complexes were isolated within the silica capsule, as indicated by the XPS experiments, and we consequently believe we have obtained nano-sized $(\text{PdO})_n$ clusters (n = ca. 12).

We further examined the conversion of the $(\text{PdO})_n$ oxide cluster to a Pd_n metal cluster by reduction with hydrogen. After heating the cluster under a hydrogen/argon atmosphere at 400 °C for 4 h, XPS analysis of the product showed the core-level Pd $3d_{3/2}$ and $3d_{5/2}$ peaks of Pd_n at 340.7 and 335.1 eV, respectively (Figure 4a). Thus, we confirmed the reduction of the PdO cluster to a Pd^0 species, which was also confirmed by XANES analysis (Figure 4c). The n value of the Pd_n cluster should be comparable to that of $(\text{PdO})_n$ (n = ca. 12), because hydrogen reduction is moderate enough to keep the capsular structure of silica and the reduction therefore occurs within the isolated hollows of the silica. Solid-state ^{29}Si NMR spectra supported that the structures of silica shell were retained after the reduction (Supporting Information, Figure S8).

In summary, we have succeeded in preparing hollow silica nanoparticles templated by a $\text{Pd}_{12}\text{L}_{24}$ spherical complex. The incarcerated $\text{Pd}_{12}\text{L}_{24}$ complex is a suitable precursor for the $(\text{PdO})_n$ and Pd_n clusters (n = ca. 12), which can be prepared in the hollows of the silica. As related spherical complexes (for example, M_6L_{12} ,^[8] $\text{M}_{18}\text{L}_{24}$,^[9] $\text{M}_{24}\text{L}_{24}$,^[10] and $\text{M}_{24}\text{L}_{48}$,^[11] M = Pd or Pt) have been efficiently synthesized by self-assembly, the present method could also be applicable to the incarceration of various metal or metal oxide clusters with predetermined, exact n values in the range of 10–20. For previous nanocluster preparation methods, values in this range have been shown to be the most difficult to control. New catalytic and physical properties for the incarcerated $(\text{PdO})_n/\text{Pd}_n$ clusters are currently under investigation.

Experimental Section

Synthesis of Sphere 2: Ligand **1** (2.23 mg, 5.00 μmol) was treated with a DMSO solution of $\text{Pd}(\text{BF}_4)_2(\text{CH}_3\text{CN})_4$ (10 mM, 0.52 mL, 5.2 μmol) at 50 °C for 1 h. The quantitative formation of sphere **2** was confirmed by ^1H NMR and CSI-MS. ^1H NMR (500 MHz, $[\text{D}_6]\text{DMSO}$, 27 °C): δ = 9.38 (br, 96H), 8.36 (br, 96H), 7.96 (br, 248H), 7.56 (br, 48H), 4.07 (br, 48H), 3.64 (br, 144H), 1.69 (br, 48H), 1.42 (br, 48H), 1.01 (br, 48H), 0.73 ppm (br, 48H).

Synthesis of $2\text{C}(\text{SiO}_2)_m$: Sphere **2** (0.024 μmol) in DMSO (80 μL , 0.30 mM) was successively diluted with MeOH (0.72 mL), D_2O (20 μL), and aqueous DNO_3 (0.33 w/w %, 2.0 μL), and then treated with tetramethoxysilane (2000 or 7200 equiv vs. **2**) at RT for 5 days. As the reaction progressed, the ^1H signals of **2** broadened, which indicated the formation of silica nanoparticles on the surface of **2** (m = 2000). After all of the $\text{Si}(\text{OCH}_3)_4$ groups were hydrolyzed,

2C $(\text{SiO}_2)_m$ was analyzed. ^1H NMR (500 MHz, $[\text{D}_6]\text{DMSO}$, 27 °C): δ = 9.28 (br, 96H), 8.15 (br, 96H), 7.95 (br, 24H), 7.48 (br, 48H), 4.09 (br, 48H), 1.80 (br, 48H), 1.55 (br, 48H), 0.63 ppm (br, 48H).

Synthesis of $(\text{PdO})_n\text{C}(\text{SiO}_2)_m$ and $\text{Pd}_n\text{C}(\text{SiO}_2)_m$: **2C** $(\text{SiO}_2)_m$ was calcinated at 400 °C for 2 h in air to afford $(\text{PdO})_n\text{C}(\text{SiO}_2)_m$. The resulting brown solids were reduced at 400 °C for 4 h under hydrogen atmosphere to afford $\text{Pd}_n\text{C}(\text{SiO}_2)_m$. The reduction was conducted under a continuous flow of H_2/Ar (10:90) at a rate of 100 mL min^{−1}. After reduction, the resulting solids were kept under Ar atmosphere to avoid oxidation by air, and analyzed.

Received: February 16, 2012

Revised: March 30, 2012

Published online: April 27, 2012

Keywords: cage-templated synthesis · hollow silica nanoparticles · nanoclusters · palladium · self-assembly

- [1] a) L. S. Ott, R. G. Finke, *Coord. Chem. Rev.* **2007**, *251*, 1075–1100; b) K. Okamoto, R. Akiyama, H. Yoshida, T. Yoshida, S. Kobayashi, *J. Am. Chem. Soc.* **2005**, *127*, 2125–2135; c) T. Mitsudome, K. Nose, K. Mori, T. Mizugaki, K. Ebitani, K. Jitsukawa, K. Kaneda, *Angew. Chem.* **2007**, *119*, 3352–3354; *Angew. Chem. Int. Ed.* **2007**, *46*, 3288–3290; d) W. E. Kaden, T. Wu, W. A. Kunkel, S. L. Anderson, *Science* **2009**, *326*, 826–829; e) K. Yamamoto, T. Imaoka, W.-J. Chun, O. Enoki, H. Katoh, M. Takenaga, A. Sonoi, *Nat. Chem.* **2009**, *1*, 397–402.
- [2] a) U. Kreibitz, M. Vollmer, *Optical Properties of Metal Clusters*, Springer, Berlin, **1995**; b) J. P. Wilcoxon, P. P. Provencio, *J. Am. Chem. Soc.* **2004**, *126*, 6402–6408; c) S. W. Han, Y. Kim, K. Kim, *J. Colloid Interface Sci.* **1998**, *208*, 272–278.
- [3] a) J. P. Bucher, D. C. Douglass, L. A. Bloomfield, *Phys. Rev. Lett.* **1991**, *66*, 3052–3055; b) I. M. L. Billas, A. Châtelain, W. A. de Heer, *Science* **1994**, *265*, 1682–1684; c) J. Bannmann, et al., *Surf. Sci. Rep.* **2005**, *56*, 189–275.
- [4] a) W. A. de Heer, *Rev. Mod. Phys.* **1993**, *65*, 611–676; b) A. Piednoir, E. Perrot, S. Granjeaud, A. Humbert, C. Chapon, C. R. Henry, *Surf. Sci.* **1997**, *391*, 19–26; c) H. Yasumatsu, T. Hayakawa, S. Koizumi, T. Kondow, *J. Chem. Phys.* **2005**, *123*, 124709–12717; d) R. Alayan, L. Arnaud, M. Broyer, E. Cottancin, J. Lermé, J. L. Vialle, M. Pellarion, *Phys. Rev. B* **2006**, *73*, 125444–125457; e) T. Wu, W. E. Kaden, W. A. Kunkel, S. L. Anderson, *Surf. Sci.* **2009**, *603*, 2764–2770.
- [5] a) J. P. Wilcoxon, B. L. Abrams, *Chem. Soc. Rev.* **2006**, *35*, 1162–1194; b) J. D. Aiken, R. G. Finke, *J. Mol. Catal. A* **1999**, *145*, 1–44.
- [6] M. Zhao, L. Sun, R. M. Crooks, *J. Am. Chem. Soc.* **1998**, *120*, 4877–4878.
- [7] a) M. Tominaga, K. Suzuki, M. Kawano, T. Kusukawa, T. Ozeki, S. Sakamoto, K. Yamaguchi, M. Fujita, *Angew. Chem.* **2004**, *116*, 5739–5743; *Angew. Chem. Int. Ed.* **2004**, *43*, 5621–5625; b) K. Suzuki, S. Sato, M. Fujita, *Nat. Chem.* **2010**, *2*, 25–29; c) K. Suzuki, K. Takao, S. Sato, M. Fujita, *Angew. Chem.* **2011**, *123*, 4960–4963; *Angew. Chem. Int. Ed.* **2011**, *50*, 4858–4861.
- [8] a) K. Suzuki, M. Tominaga, M. Kawano, M. Fujita, *Chem. Commun.* **2009**, 1638–1640; b) D. Fujita, A. Takahashi, S. Sato, M. Fujita, *J. Am. Chem. Soc.* **2011**, *133*, 13317–13319.
- [9] Q.-F. Sun, S. Sato, M. Fujita, *Nat. Chem.* **2012**, *4*, 330–333.
- [10] Q.-F. Sun, T. Murase, S. Sato, M. Fujita, *Angew. Chem.* **2011**, *123*, 10502–10505; *Angew. Chem. Int. Ed.* **2011**, *50*, 10318–10321.
- [11] Q.-F. Sun, J. Iwasa, D. Ogawa, Y. Ishido, S. Sato, T. Ozeki, Y. Sei, K. Yamaguchi, M. Fujita, *Science* **2010**, *328*, 1144–1147.